

# Gradient measure and extended self-similarity of the cosmic microwave background anisotropy

A. Bershadskii<sup>1,2</sup> and K.R. Sreenivasan<sup>2</sup>

<sup>1</sup>ICAR, P.O. Box 31155, Jerusalem 91000, Israel

<sup>2</sup>International Center for Theoretical Physics, Strada Costiera 11, I-34100 Trieste, Italy

Using the WMAP cosmic microwave background data it is shown that collisions between Alfvén wave packets and the cascades generated by these collisions (the Iroshnikov model) can determine the photon temperature fluctuations for arcminute scales on the last scattering surface.

PACS numbers: 52.40.Db, 98.80.Cq, 98.70.Vc

Cosmic electromagnetic fields are expected to be generated by the cosmological phase transitions (electroweak and QCD) in a wide interval of scales [1]-[15] before the recombination time. At earliest times, the magnetic fields are generated by particle physics processes, with length scales typical of particle physics. It is shown in [1] that turbulence with its cascade processes is operative, and hence the scale of magnetic fields is considerably larger than would be the case if turbulence were ignored. In particular, it is shown in [3],[4],[6] that rotational velocity perturbations, induced by a tangled magnetic field can produce significant angular scale anisotropies in cosmic microwave background (CMB) radiation through the Doppler effect. The conclusions are relevant to arcminute scales [3]. For very large cosmological scales (larger than  $10^\circ$ ), on the other hand, the Anderson localization can make it impossible for the electromagnetic fields to propagate [16]. Magnetohydrodynamic (MHD) turbulence is characterized by a competition of two processes, Alfvén wave packets collisions and swirling motions. It is known [4] that on the last scattering surface the nonlinear Alfvén wave mode survives photon (Silk) damping on the arcminute scales, while the general swirling motions (as well as the compressional modes) are effectively dissipated on these scales (it is significant for further consideration that the Alfvén wave modes induce specific rotational velocity perturbations on the last scattering surface [3],[4],[6],[17]). Therefore, the cosmic baryon-photon fluid becomes dominated by Alfvén waves on the arcminute scales just before the recombination time. In the present paper we will show that specific statistical properties of such Alfvén wave dominated fluctuations are consistent with the new (WMAP) arcminute CMB data.

The incompressible magnetohydrodynamic equations can be written in terms of the Elsässer variables

$$\mathbf{z}^\pm = \mathbf{v} \pm \mathbf{B} \quad (1)$$

as

$$\partial_t \mathbf{z}^\pm + \mathbf{z}^\mp \cdot \nabla \mathbf{z}^\pm = -\nabla P + \nu_+ \Delta \mathbf{z}^\pm + \nu_- \Delta \mathbf{z}^\mp, \quad (2)$$

where  $\nu_+ = \frac{1}{2}(\nu + \eta)$ ,  $\nu_- = \frac{1}{2}(\nu - \eta)$ ,  $P$  is the total pres-

sure,  $\nu$  and  $\eta$  are coefficients of hydro and magnetic diffusion respectively. The equations are given in convenient nondimensional form using units  $B/B_0 \rightarrow B$ ,  $u/u_0 \rightarrow u$ ,  $u_0 = B_0/(4\pi\rho)^{1/2}$  and  $B_0$  is a typical magnetic field intensity.

Scaling of the structure functions of the Elsässer variables

$$\langle |\mathbf{z}^\pm(\mathbf{x} + \mathbf{r}) - \mathbf{z}^\pm(\mathbf{x})|^p \rangle \sim r^{\zeta_p} \quad (3)$$

is used as an effective tool to study their dynamics.

A first attempt to describe magnetic turbulence dominated by Alfvén waves was made in [19]. In the incompressible fluid, any magnetic perturbation propagates along the magnetic field line. Since wave packets are moving along the magnetic field line, there are two possible directions for propagation. If all the wave packets are moving in one direction, then they are stable. Therefore, the energy cascade occurs only when the opposite-travelling wave packets collide, and only collisions between similar size packets are taken into account in the Iroshnikov model. The following amount of energy:  $\Delta E \sim (v_l^3/l)(l/V_A)$  is released at collision of the two wave packets of the same size  $l$ . The energy change per collision and the duration of the collision are respectively  $v_l^2(v_l/V_A)$  and  $\Delta t \sim l/V_A$ , where  $V_A$  is the Alfvén speed. Total number of collisions for the cascade can be estimated as  $v^2/\Delta E$ . Hence, the energy cascade time  $\tau_l$  is

$$\tau_l \sim (v^2/\Delta E)^2 \Delta t \sim \frac{l}{v_l} \frac{V_A}{v_l}. \quad (4)$$

That is the cascade time is  $(V_A/v_l)$  times longer than the eddy turnover time  $(l/v_l)$ . The constancy of energy cascade,  $(v_l^4)/(lV_A) = \text{constant}$ , is assumed in the model, which results in

$$v_l^4 \sim l. \quad (5)$$

It then follows from (4) and (5)

$$\tau_l \sim l^{1/2}. \quad (6)$$

There exists a general representation for  $\zeta_p$  (3) [20]

$$\zeta_p = p/g(1-x) + C_0[1 - (1-x/C_0)^{p/g}],$$

where  $g$  is related to the basic scaling  $\delta v_l \sim l^{1/g}$  (in the Iroshnikov model (5) gives  $g = 4$ ),  $x$  is the scaling of dynamic time scale of the most intermittent structures,  $\tau_l \sim l^x$  (in the Iroshnikov model (6) gives  $x = 1/2$ ),  $C_0$  is the co-dimension of these structures with the spatial dimension  $d$ ,  $C_0 = 3 - d$  (in the Iroshnikov model these structures are known to be micro-sheets, i.e.  $d = 2$  and, consequently,  $C_0 = 1$ ). Then, for the Alfvén wave dominated model [21]

$$\zeta_p = \frac{p}{8} + 1 - (1/2)^{p/4}. \quad (7)$$

It is very significant that for this model  $\zeta_4 = 1$  (cf. basic scaling (5)). Using this fact, the so-called extended self-similarity (ESS) can be introduced in the form [21]

$$\langle |\mathbf{z}^\pm(\mathbf{x} + \mathbf{r}) - \mathbf{z}^\pm(\mathbf{x})|^p \rangle \sim \langle |\mathbf{z}^\pm(\mathbf{x} + \mathbf{r}) - \mathbf{z}^\pm(\mathbf{x})|^4 \rangle^{\zeta_p}. \quad (8)$$

The remarkable property of the ESS is that the multi-scaling (8) can survive even if the original multiscaling (3) does not exist. Due to the local (small-scale) isotropy of the fluctuations in the model we suppose that the ESS has the same  $\zeta_p$  for any vector component of the space difference:  $\mathbf{z}^\pm(\mathbf{x} + \mathbf{r}) - \mathbf{z}^\pm(\mathbf{x})$ .

We use the ESS and the model (7) to check whether the cosmic microwave background (CMB) data, obtained recently by the WMAP space mission, support the Alfvén wave domination on the arcminute scales (cf Introduction). For this purpose we calculated moments  $\langle \Delta T_r^p \rangle$ , for the space differences of the CMB temperature fluctuations  $\Delta T_r = |T(\mathbf{x} + \mathbf{r}) - T(\mathbf{x})|$ , and then checked the multiscaling

$$\langle \Delta T_r^p \rangle \sim \langle \Delta T_r^4 \rangle^{\zeta_p} \quad (9)$$

(cf. (8)).

The motion of the scatterers imprints a temperature fluctuation,  $\delta T$ , on the CMB through the Doppler effect [3],[4] (see also [6] and [17])

$$\frac{\delta T(\mathbf{n})}{T} \sim \int g(L) \mathbf{n} \cdot \mathbf{v}_b(\mathbf{x}) dL$$

where  $\mathbf{n}$  is the direction (the unit vector) on the sky,  $\mathbf{v}_b$  is the velocity field of the baryons evaluated along the line of sight,  $\mathbf{x} = L\mathbf{n}$ , and  $g$  is the so-called visibility. It should be noted that, in a potential flow, waves perpendicular to the line of sight lack a velocity component parallel to the line of sight; consequently, generally there is no Doppler effect for the potential flows. The same is not true for vortical flows, since the waves that run perpendicular to the line of sight have velocities parallel to the line of sight [22] (see [3],[4] about the rotational velocity perturbations induced by the Alfvén-wave modes on the last scattering surface). One can look at the modulation from another (though similar) point of view [6]. In

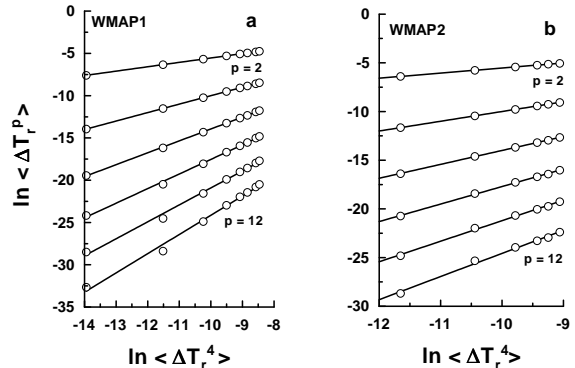


FIG. 1: **a**: Logarithm of moments of different orders  $\langle |\Delta T_r|^p \rangle$  against logarithm of  $\langle |\Delta T_r|^4 \rangle$  for the cleaned and Wiener-filtered WMAP1 data set. The straight lines (the best fit) are drawn to indicate the scaling (9); **b**: the same as in figure 1a but for WMAP2 data set.

general, vector perturbations of the metric have the form

$$(h_{\mu\nu}) = \begin{pmatrix} 0 & B_i \\ B_j & H_{i,j} + H_{j,i} \end{pmatrix},$$

where  $\mathbf{B}$  and  $\mathbf{H}$  are divergence-free, 3D vector fields supposed to vanish at infinity. The authors of [6] introduced two gauge invariant quantities

$$\sigma = \dot{\mathbf{H}} - \mathbf{B} \quad \text{and} \quad \mathbf{z}_- = \mathbf{v} - \mathbf{B}$$

which represent the vector contribution to the perturbation of the extrinsic curvature and the vorticity (cf. (6) and (13)). The general form of the CMB temperature fluctuations produced by vector perturbations is [6]

$$\left( \frac{\delta T}{T} \right)^{(vec)} = -\mathbf{Z}_- \cdot \mathbf{n} \Big|_{t_{dec}}^{t_0} + \int_{t_{dec}}^{t_0} \dot{\sigma} \cdot \mathbf{n} dL$$

where  $\mathbf{Z}_- = \mathbf{z}_- - \sigma$  is a gauge-invariant generalization of the velocity field, and the subscripts  $dec$  and  $0$  denote the decoupling epoch ( $z_{dec} \gg 1100$ ) and today respectively. We see from this equation that, besides the Doppler effect, Alfvén waves give rise to an integrated Sachs-Wolfe term. However, since the geometric perturbation  $\sigma$  decays with time, the integrated term is dominated by its lower boundary and just cancels  $\sigma$  in  $\mathbf{Z}_-$ .

We used the WMAP data cleaned from foreground contamination and Wiener filtered [23] (the original temperature is given in  $\mu K$  units). Wiener filtering suppresses the noisiest modes in a map and shows the signal that is statistically significant. However, even after the cleaning and filtering some data points with the largest magnitudes seem to be suspicious. Therefore, we also made several magnitude-threshold cutoffs to check the stability of our calculations to these cutoffs.

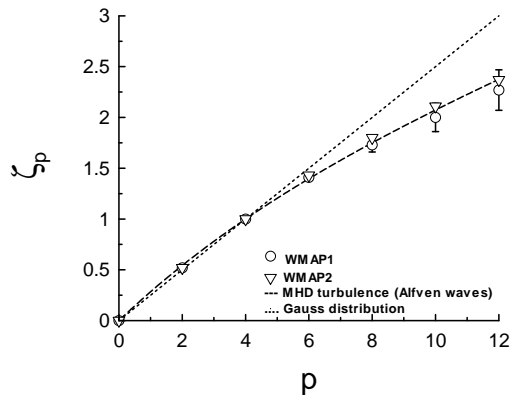


FIG. 2: The scaling exponents  $\zeta_p$ , corresponding to the WMAP data (circles - WMAP1, triangles - WMAP2). The dotted straight line corresponds to the Gaussian distributions and the dashed curve corresponds to the Alfvén-wave dominated model calculations (7).

Figure 1a shows the results of the calculations in the form suitable for the multiscaling of the type (9). The straight lines in this figure (the best fits) correspond to the multiscaling (9). The cutoff in this case excluded about 1% of the data points (we will call this data set WMAP1). Figure 1b shows analogous data with a cutoff which excluded about 10% of the data points (we will call this data set WMAP2).

Figure 2 shows the exponents  $\zeta_p$  (open circles correspond to WMAP1 data set and triangles to WMAP2) extracted from figures 1a,b as slopes of the straight lines. We also show in figure 2 as dotted line the dependence of  $\zeta_p$  on  $p$  for the Gaussian distributions ( $\zeta_p = p/4$  for any Gaussian distribution), and we show the model dependence (7) as dashed line.

One can see that starting from  $p \simeq 6$  the data depart systematically from the Gaussian straight line and follow quite closely to the model curve (indicated by the dashed line) predicted for the Alfvén-wave dominated turbulence (7).

To give an additional support to the correspondence just noted between the WMAP data and the Alfvén wave dominated model, let us introduce a gradient measure for the cosmic microwave radiation temperature  $T$  fluctuations

$$\chi_r = \frac{\int_{v_r} (\nabla T)^2 dv}{v_r} \quad (10),$$

where  $v_r$  is a subvolume with space-scale  $r$ . Scaling laws of this measure, such as

$$\frac{\langle \chi_r^p \rangle}{\langle \chi_r \rangle^p} \sim r^{-\mu_p} \quad (11)$$

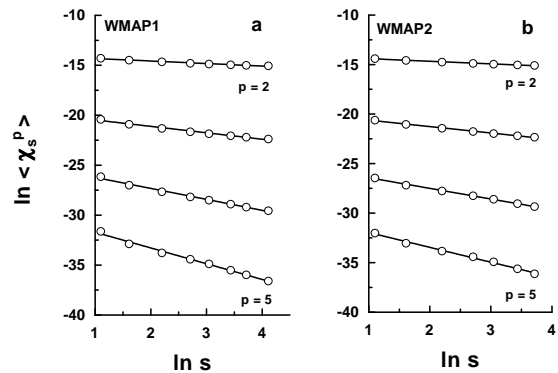


FIG. 3: **a**: Logarithm of the temperature gradient moments  $\langle \chi_s^p \rangle$  calculated for the WMAP1 data set against  $\ln s$ . The straight lines (the best fit) are drawn to indicate the scaling in the log-log scales; **b**: the same as in figure 3a but for WMAP2 data set.

are an important characteristic of the temperature dissipation rate [24]. The exponents  $\mu_p$  can be related [24] to the exponents  $\zeta_p$  by the equation

$$\mu_p = 1 - \zeta_{4p} \quad (12)$$

that allows us to check the model equation (7) also through the scaling (11) of the moments of the gradient measure.

Technically, using the cosmic microwave pixel data map, we will calculate the cosmic microwave radiation temperature gradient measure using summation over pixel sets instead of integration over subvolumes  $v_r$ . The multiscaling of type (11) (if exists) will be then written as

$$\frac{\langle \chi_s^p \rangle}{\langle \chi_s \rangle^p} \sim s^{-\mu_p} \quad (13)$$

where the metric scale  $r$  is replaced by number of the pixels,  $s$ , characterizing the size of the summation set. The  $\chi_s$  is a surrogate of the real 3D dissipation rate  $\chi_r$ . It is believed that the surrogates can reproduce quantitative multiscaling properties of the dissipation rate [24]. Since in our calculations  $\langle \chi_s \rangle$  is independent of  $s$ , we will calculate the exponents  $\mu_p$  directly from the scaling of  $\langle \chi_s^p \rangle$ .

Figure 3a shows scaling of the CMB temperature gradient moments  $\langle \chi_s^p \rangle$  calculated for the WMAP1 map. The straight lines (the best fit) are drawn to indicate the scaling in log-log scales. Figure 3b shows the results of analogous calculations produced for WMAP2 data set.

Figure 4 shows the exponents  $\mu_p$  extracted from figure 3a (circles) and from figure 3b (triangles). Dashed line in figure 4 corresponds to the model calculations (eqs.

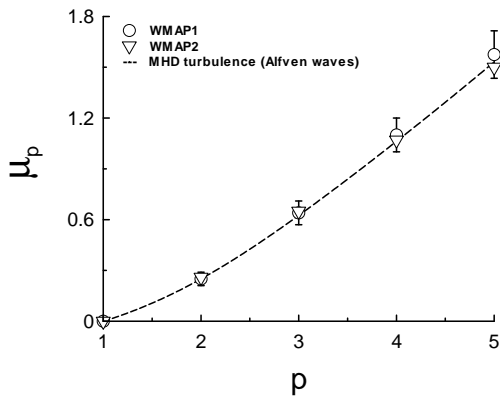


FIG. 4: The scaling exponents  $\mu_p$  corresponding to the WMAP1 data set (circles) and for the WMAP2 data set (triangles). The dashed curve corresponds to the Alfven -wave dominated model calculations (7),(12).

(7),(12)).

The results presented in the paper can be considered as a tentative indication of the existence [1]-[15] of the considerable magnetic fields at the recombination time. The extended self-similarity (figure 2) shows clear non-Gaussian character of the high moments which, together with the closeness of the low moments to the Gaussian behavior, can shed light on the longstanding discussion about Gaussianity of the small-scale cosmological fluctuations. The theoretically predicted survival of the Alfven waves on the last scattering surface at the arcminute scales and, moreover, domination of their interactions (the cascade collisions of the Alfven wave packets) on these scales can be also considered now rather plausible. WMAP sky maps produced by the WMAP team were analyzed by the team itself. They found the CMB temperature *fluctuations* (i.e.  $\delta T = T - \langle T \rangle$ ) to obey Gaussian statistics [25]. Analogous situation occurs in fluid turbulence (near-) Gaussianity of velocity fluctuations and non-Gaussian multiscaling of the corresponding space *increments* [26],[27]. The (near-) Gaussianity of a random field fluctuations themselves does not contradict to a pronounced non-Gaussian multiscaling of corresponding increments of the field, which can be seen for sufficiently high order moments. This takes place in classic fluid turbulence for velocity field and, apparently, for the CMB temperature fluctuations (probably just due to turbulence modulation). In particular, it was shown for fluid turbulence [26],[27] that knowledge about the spectrum for the Gaussian processes is certainly insufficient to reproduce the observed multiscaling of the increments. We suppose that there are two reasons why the previous studies of the CMB maps failed to detect

the non-Gaussianity: using the fluctuations of the temperature (not their space increments, (9)) and the fact that non-Gaussianity does not make its appearance in the ESS up to the 6 moment even if space increments are considered.

Finally, it should be noted that we cannot exclude other contributions to high-order structure functions which may be produced by non-linear effects due to gravity (e.g. the Rees-Sciama effect), but the good quantitative correspondence to turbulence (both for the structure functions and for the gradient measure), observed in the figures 2 and 4, indicates that the turbulence may be a dominating factor here.

The authors are grateful to C.H. Gibson for discussions, and to Tegmark's group and to the NASA Goddard Space Flight Center for providing the data.

- 
- [1] A. Brandenburg, K. Enqvist and P. Olesen, Phys. Rev. D, **54**, 1291 (1996).
  - [2] J.D. Barrow, P.G. Ferreira and J. Silk, Phys. Rev. Lett., **78**, 3610 (1997).
  - [3] K. Subramanian and J.D. Barrow, Phys. Rev. Lett., **81**, 3575 (1998).
  - [4] K. Subramanian and J.D. Barrow. Phys. Rev. D, **58**, 083502 (1998).
  - [5] K. Jedamzik, V. Katalinic, and A.V. Olinto, Phys. Rev. D, **57**, 3264 (1998).
  - [6] R. Durrer, T. Kahniashvili, and A. Yates, Phys. Rev. D, **58**, 123004 (1998).
  - [7] M. Christensson, M. Hindmarsh and A. Brandenburg, Phys. Rev. E, **64**, 056405 (2001).
  - [8] D. Grasso and H.R. Rubinstein, Phys. Rept., **348**, 163 (2001).
  - [9] A. Kosowsky, A. Mack, and T. Kahniashvili, Phys. Rev. D, **66**, 024030 (2002).
  - [10] A.D. Dolgov and D. Grasso, Phys. Rev. Lett., **88**, 011301 (2002).
  - [11] A.D. Dolgov, D. Grasso and A. Nicolis, Phys. Rev. D, **66**, 103505 (2002).
  - [12] M. M. Forbes and A. Zhitnitsky, Phys. Rev. Lett., **85**, 5268 (2000).
  - [13] M. M. Forbes and A. Zhitnitsky, hep-ph/0102158 (2001).
  - [14] D.T. Son, Phys. Rev. D, **59**, 063008 (1999).
  - [15] J.M. Cornwall, Phys. Rev. D, **56**, 6146 (1997).
  - [16] A. Bershadskii, Phys. Lett. B, **559** (2003) 107.
  - [17] J. Adams, U.H. Danielsson, D. Grasso and H. Rubinstein, Phys. Lett. B, **388**, 253 (1996).
  - [18] Parker, E. N., *Cosmic Magnetic Fields*, Clarendon Press, Oxford (1979).
  - [19] P. Iroshnikov, Astron. Zh. **40**, 742 (1963) (English transl.: Sov. Astron. 7, 566 (1964)).
  - [20] H. Politano and A. Pouquet, Phys. Rev., E, **52**, 636 (1995).
  - [21] R. Grauer, J. Krug and C. Marliani, Phys. Lett. A, **195** 335 (1994).
  - [22] J.P. Ostriker and E.T. Vishniac, ApJ, **306**, L51 (1986).
  - [23] M. Tegmark, A. de Oliveira-Costa, A. Hamilton,

astro-ph/0302496.

- [24] K.R. Sreenivasan, *Annu. Rev. F. Mech.* **23**, 539 (1991).
- [25] C.L. Bennet et al, 2003, *ApJ. Suppl.*, **148**, 1.
- [26] A. Juneja et al. 1994, *Phys. Rev. E*, **49**, 5179.
- [27] G. Stolovitzky and K.R. Sreenivasan 1994, *Rev. Mod. Phys.*, **66**, 229.